NASA TECHNICAL NOTE

NASA TN D-6361

COMPARISON OF NONCAVITATION AND CAVITATION PERFORMANCE FOR 78°, 80.6°, AND 84° HELICAL INDUCERS OPERATED IN HYDROGEN

by Royce D. Moore and Phillip R. Meng

Lewis Research Center
Cleveland, Ohio 44135

NATIONAL AERONAUTICS AND SPACE ADMINISTRATION • WASHINGTON, D. C. • MAY 1971

1. Report No.	2. Government Accession No.	3. Recipient's Catalog No.
NASA TN D-6361		

4. Title and Subtitle: COMPARISON OF NONCAVITATION AND CAVITATION PERFORMANCE FOR 78°, 80.6°, AND 84° HELICAL INDUCERS OPERATED IN HYDROGEN

5. Report Date: May 1971

6. Performing Organization Code:

7. Author(s): Royce D. Moore and Phillip R. Meng

8. Performing Organization Report No.: E-5972

10. Work Unit No.: 128-31

9. Performing Organization Name and Address:
Lewis Research Center
National Aeronautics and Space Administration
Cleveland, Ohio 44135

11. Contract or Grant No.:

13. Type of Report and Period Covered: Technical Note

12. Sponsoring Agency Name and Address:
National Aeronautics and Space Administration
Washington, D.C. 20546

14. Sponsoring Agency Code:

15. Supplementary Notes:

16. Abstract

Three different helical inducers were tested in liquid hydrogen. The tip helical angles were 78°, 80.6°, and 84°. The pressure requirements as well as the thermodynamic effects of cavitation for a head-rise coefficient ratio of 0.70 were the greatest for the 84° inducer and least for the 78° inducer for a given flow coefficient ratio. The noncavitating flow range was the greatest for the 78° inducer and least for the 84° inducer.

17. Key Words (Suggested by Author(s)): Hydrogen; Inducers; Cavitation

18. Distribution Statement: Unclassified - unlimited

19. Security Classif. (of this report)	20. Security Classif. (of this page)	21. No. of Pages	22. Price*
Unclassified	Unclassified	24	$3.00

*For sale by the National Technical Information Service, Springfield, Virginia 22151

COMPARISON OF NONCAVITATION AND CAVITATION PERFORMANCE FOR 78°, 80.6°, AND 84° HELICAL INDUCERS OPERATED IN HYDROGEN

by Royce D. Moore and Phillip R. Meng

Lewis Research Center

SUMMARY

Measured required net positive suction head was used in conjunction with a semiempirical prediction method to predict the thermodynamic effects of cavitation for a 78° helical inducer. The thermodynamic effects were compared with values obtained for 84° and 80.6° helical inducers. The noncavitating and cavitating performances of the three inducers were also compared. These experimental inducers were tested over a liquid temperature range of 15.5 to 22.3 K (27.9° to 40.1° R) and a flow coefficient range of 0.058 to 0.130. The magnitude of the thermodynamic effects of cavitation as well as the pressure requirements were the greatest for the 84° inducer and least for the 78° inducer for a given flow coefficient ratio. The noncavitating flow range was the greatest for the 78° inducer and least for the 84° inducer. The noncavitating head-rise coefficient decreased with increasing flow coefficient.

INTRODUCTION

The turbopump of a liquid rocket engine must be capable of operating with low tank pressure in order to minimize tank weight. To provide this capability, the turbopump generally employs an inducer stage ahead of the main rotor. The results of reference 1 indicate that the flow rate of the flat-plate helical inducers can be increased by decreasing the blade helical angle.

The inducers used in rocket engines are capable of satisfactory operation at relatively low inlet pressures because of their ability to tolerate considerable amounts of cavitation. The required net positive suction head NPSH for an inducer operated at a given cavitating performance level has been shown to vary with the liquid, the liquid

temperature, the blade geometry, and the rotative speed and flow rate at which the inducer is operated (refs. 2 to 8). This variation in NPSH requirements has been attributed, in part, to the thermodynamic effects of cavitation resulting from the varying degrees of evaporative cooling. This cooling lowers the vapor pressure in the cavity which lowers, by the same amount, the NPSH requirements. Venturi cavitation studies (ref. 9) have shown that the magnitude of the thermodynamic effects of cavitation also depend on the surface pressure distribution, that is, the local liquid velocities and pressures that influence the heat- and mass-transfer rates.

Variation in blade leading edge fairing and thickness, blade shape, and blade angle will affect the pressure distribution on the blade suction surface and thus should affect the magnitude of the thermodynamic effects of cavitation. In reference 8, it was shown that the thermodynamic effects varied with blade leading-edge thickness; and, in reference 6, the thermodynamic effects were shown to vary with blade shape. In the present study, changes in blade helical angle and its interrelated effect on leading-edge fairing are considered.

In previous investigations, the cavitation performances of an 84° (ref. 2) and an 80.6° (ref. 7) helical inducer were determined in liquid hydrogen. The thermodynamic effects of cavitation varied considerably between the two inducers. In reference 10, the cavitation performance for a 78° helical inducer operated in hydrogen was presented.

The objectives of this investigation are to determine the thermodynamic effects of cavitation for the 78° helical inducer and to compare these values with those obtained for the 80.6° and 84° helical inducers. The noncavitation and cavitation performances of the three inducers are also compared. The experimental inducers were tested in liquid hydrogen. The liquid temperature ranged from 15.5 to 22.3 K (27.9° to 40.1° R). The flow coefficient range varied with inducer and ranged from 0.058 for the 84° inducer to 0.130 for the 78° inducer.

APPARATUS AND PROCEDURE

Test Inducers

The three experimental inducers used in this investigation were designed in a similar manner. Each rotor was a three-bladed, flat-plate helical inducer with a nominal tip diameter of 12.70 centimeters (5.0 in.). The rotors were made of 6061-T6 aluminum. A photograph of each inducer is presented in figure 1, and the significant geometric features are given in table I. The blade leading edges were faired on the suction surfaces at an angle equal to one-half the complement of the blade helical angle (see

fig. 2). Since the blade fairing angle is directly related to the blade helical angle, the combined effects will be referred to herein as blade helical angle effects.

Test Facility

This investigation was conducted in the liquid-hydrogen pump test facility shown schematically in figure 3. The facility is basically the same as that described in references 2, 9, 10, and 11. However, after the tests of reference 2 (84° helical inducer), the facility was modified to allow testing up to 30 000 rpm in order to evaluate cavitation performance at higher liquid temperatures. The inducers were installed in an inlet line that was located near the bottom of the 9.5-cubic-meter (2500-gal) vacuum-jacketed research tank. A booster rotor located downstream of the inducer was used to overcome system losses. The flow path is down the inlet line, through the inducer and booster rotor to a collector scroll, and into the discharge line to the storage dewar.

Test Procedure

The research tank was filled with liquid hydrogen from the storage tank. Before each cavitation test, the hydrogen in the research tank was conditioned to the desired liquid temperature. The tank was then pressurized to 10.4 newtons per square centimeter (15 psi) above the vapor pressure. When the test rotative speed was attained, the tank pressure (NPSH) was slowly reduced until the head rise deteriorated because of cavitation. The flow rate, rotative speed, and bulk liquid temperature were maintained essentially constant during each test. The noncavitating performance was obtained by varying the flow rate while maintaining a constant rotative speed and liquid temperature. The tank pressure for the noncavitating runs was maintained at 10.4 newtons per square centimeter (15 psi) above vapor pressure.

Instrumentation

The location of the instrumentation used in this investigation is shown schematically in figure 4. The measured parameters and estimated system errors are also listed in this figure.

The vapor pressure was measured with a vapor pressure bulb that was charged with hydrogen from the research tank. The vapor pressure bulb was located at the entrance of the inlet line. Tank pressure, measured in the ullage space, was used as the refer-

ence pressure for the differential pressure transducers. The liquid level above the inducer was added to the reference pressure to correct the differential pressures to the inducer inlet conditions. An averaged hydrogen temperature at the inducer inlet was obtained from two platinum resistor thermometers. A shielded total-pressure probe located at midstream approximately 2.5 centimeters (1 in.) downstream of the test rotor was used to measure inducer pressure rise. Pump flow rate was obtained with a venturi flowmeter that was calibrated in water.

The differential pressure measured directly between tank pressure and the vapor bulb at the entrance to the inlet line was converted to meters (ft) of head to obtain tank NPSH. (All symbols are defined in the appendix.) Inducer NPSH was obtained by subtracting the inlet line losses from the tank NPSH. The losses were calculated by multiplying the inlet line fluid velocity head by the entrance loss coefficient, which was determined from air calibrations.

RESULTS AND DISCUSSION

The cavitation performance and thermodynamic effects of cavitation were presented in reference 7 for the 80.6° helical inducer and in reference 2 for the 84° helical inducer. The cavitation performance of the 78° helical inducer was presented in reference 10. The thermodynamic effects of cavitation will be calculated for the 78° helical inducer using the prediction method of reference 6. The thermodynamic effects of cavitation for the 84° helical inducer as presented in reference 2 were based on slightly different exponents in the prediction equation than those of reference 6. Thus, the thermodynamic effects will be recomputed for the 84° helical inducer.

Thermodynamic Effects of Cavitation

Prediction method. - A method for predicting the thermodynamic effects of cavitation and the cavitation performance of inducers is presented in detail in reference 6. A brief resumé of the prediction method is also presented herein. In reference 6, a heat balance between the heat required for vaporization and the heat drawn from the liquid adjacent to the cavity is used to show that the cavity pressure depression (below free-stream vapor pressure) is

$$\Delta h_v = \left(\frac{\rho_v}{\rho_l}\right)\left(\frac{L}{C_l}\right)\left(\frac{dh_v}{dT}\right)\left(\frac{\gamma_v}{\gamma_l}\right) \tag{1}$$

With the properties of the fluid known, values of vapor- to liquid-volume ratio of $\forall_v/\forall_l$ as a function of Δh_v can be obtained by numerical integration of equation (1). This takes into account changes in properties as the equilibrium temperature drops because of the evaporative cooling. The calculated depression in vapor pressure Δh_v is plotted as a function of $\forall_v/\forall_l$ for a range of liquid hydrogen temperatures in figure 5. Equation (1) cannot be used directly to predict the required NPSH because the absolute value of $\forall_v/\forall_l$ is not known. However, it was shown that, if a reference value of $\forall_v/\forall_l$ is established experimentally by determining Δh_v at a given set of operating conditions, values of $\forall_v/\forall_l$ relative to this reference value can be estimated from the following equation:

$$\frac{\forall_v}{\forall_l} = \left(\frac{\forall_v}{\forall_l}\right)_{ref} \left(\frac{\alpha_{ref}}{\alpha}\right) \left(\frac{N}{N_{ref}}\right)^{0.8} \tag{2}$$

This equation assumes geometrically similar cavitating flow conditions (i.e., the same flow coefficient ϕ and the same head-rise-coefficient ratio ψ/ψ_{NC} for the predicted condition as for the reference condition).

The equation for predicting the inducer cavitation performance for a constant flow coefficient and head-rise-coefficient ratio is repeated (from ref. 6) for convenience:

$$\frac{NPSH + \Delta h_v}{NPSH_{ref} + (\Delta h_v)_{ref}} = \left(\frac{N}{N_{ref}}\right)^2 \tag{3}$$

This relation requires that values of NPSH and N for two experimental test points be available for the inducer of interest. These experimental data can be for any combination of liquid, liquid temperature, or rotative speed, provided that at least one set of data exhibits a measurable thermodynamic effect. From these experimental data, the cavitation performance for the inducer can be predicted for any liquid, liquid temperature, or rotative speed.

78° helical inducer. - The required NPSH for a head-rise-coefficient ratio of 0.70 is plotted in figure 6 as a function of flow coefficient for several hydrogen temperatures. These data are from reference 10. The required NPSH for a rotative speed of 25 000 rpm is presented in figure 6(a) and that for a rotative speed of 30 000 rpm is presented in figure 6(b). The required NPSH for a rotative speed of 30 000 rpm and liquid temperatures of 20.3 and 21.7 K (36.5° and 39.1° R) were used as the two experimental reference curves (solid lines) to calculate the thermodynamic effects of cavitation.

A comparison between the predicted and experimental values of required NPSH is also shown in figure 6. The experimental values of required NPSH compare reasonably well with the predicted curves for all liquid temperatures tested at a rotative speed of 30 000 rpm and for 20.3 K (36.5° R) at a rotative speed of 25 000 rpm. For the higher temperatures at 25 000 rpm, the experimental values are less than the predicted values. This trend has been observed for other inducers when the required NPSH is near the velocity head. The predicted curves are also shown for 13.8 K (24.9° R) hydrogen. At that temperature, the thermodynamic effects should be zero, and the required NPSH should be the same as that required for cold water operated in this inducer.

The predicted magnitude of the thermodynamic effects of cavitation for the 78° helical inducer is shown in figure 7. The thermodynamic effects increased with both increasing liquid temperature and rotative speed. They also increased with increasing flow coefficient. The magnitude of the thermodynamic effects ranged from about 4 meters (13 ft) to about 33.5 meters (110 ft) over the ranges of temperature, speed, and flow coefficient tested.

84° helical inducer. - As previously indicated, the thermodynamic effects will be recalculated for the 84° helical inducer using the prediction method presented herein (eq. (2)). The exponents are slightly different from those presented in reference 2. The required NPSH for a head-rise-coefficient ratio of 0.70 is plotted in figure 8 as a function of flow coefficient. Several liquid temperatures are shown for a rotative speed of 20 000 rpm. The required NPSH for liquid temperatures of 15.5 and 17.2 K (27.9° and 30.9° R) were used as the experimental reference curves to calculate the required NPSH at the other temperatures and the thermodynamic effects of cavitation (fig. 9). Reasonable agreement between predicted (dashed lines) and experimental values of required NPSH was obtained.

The predicted magnitude of the thermodynamic effects of cavitation are shown in figure 9 for the 84° helical inducer. The Δh_v curves presented are for a rotative speed of 20 000 rpm and a head-rise-coefficient ratio of 0.70. The thermodynamic effects of cavitation increased with increasing liquid temperature and decreased with increasing flow coefficient. The predicted thermodynamic effects are less than 3.0 meters (10 ft) greater than those presented in reference 2.

80.6° helical inducer. - A comparison of predicted and measured values of required NPSH as well as the thermodynamic effects of cavitation for the 80.6° helical inducer were presented in reference 7. They are repeated herein for easy reference. The required NPSH is presented in figure 10, and the thermodynamic effects in figure 11. For a rotative speed of 30 000 rpm (fig. 10(b)), good agreement is shown between the predicted and measured NPSH; but, for a rotative speed of 25 000 rpm (fig. 10(a)), the predicted values are slightly greater than the measured values.

The thermodynamic effects of cavitation (fig. 11) increased with increasing liquid temperature and rotative speed, but decreased with increasing flow coefficient.

Comparison of Inducers

Noncavitating performance. - The noncavitating head-flow characteristics of the three inducers are compared in figure 12 where head-rise-coefficient ψ is plotted as a function of flow coefficient φ. The flow ranges for the 80.6° and 78° helical inducers are nearly the same, and both ranges were wider than for the 84° inducer. However, as indicated in reference 10, the maximum flow of the 78° helical inducer was limited by the system resistance. The 78° inducer, therefore, should have a greater flow range than the 80.6° inducer. The negative slope of the head-flow curves is more pronounced at the higher helical angles. The noncavitating trends observed for these inducers in hydrogen were the same as those observed for similar inducers in water (ref. 1).

Cavitating performance. - Some general trends of cavitation performance are observed, even though no direct comparison can be made from figures 6, 8, and 10. For all three inducers, the required NPSH increased with increasing flow coefficient and decreased with increasing liquid temperature. For both the 78° and 80.6° inducers (which were tested at two speeds), the required NPSH increased with increasing rotative speed.

Thermodynamic effects of cavitation. - Direct comparison of the thermodynamic effects of cavitation of figures 7, 9, and 11 cannot be made because the 84° inducer was tested at 20 000 rpm and the other two inducers were tested at 25 000 and 30 000 rpm. The thermodynamic effects increased with increasing liquid temperature for all three inducers. For the 80.6° and 84° inducers the thermodynamic effects decreased with increasing flow coefficient. The 78° inducer showed the opposite trend with thermodynamic effects increasing with flow coefficient. For both the 78° and 80.6° helical inducers, the thermodynamic effects of cavitation were greater for 30 000 rpm than for 25 000 rpm.

Cavitation parameters. - Cavitation performance, as measured by both the required NPSH and the magnitude of the thermodynamic effects of cavitation, varies with liquid, liquid temperature, rotative speed, flow coefficient, and inducer design. Thus, when values of NPSH and Δh_v are quoted, they must be accompanied by each of the above variables.

In reference 8, two cavitation parameters were developed that allow qualitative evaluation of the cavitation performance of inducers. Comparisons are made for given values of flow coefficient and head-rise coefficient ratio. The effect of changes in liquid,

liquid temperature, and rotative speed are included in these parameters. Thus, comparisons of the cavitation parameters for the three inducers studied can be made.

A more convenient way to express the cavitation performance is to rewrite equation (3) in the following manner:

$$\text{K-factor} = \frac{\text{NPSH} + \Delta h_v}{\frac{V^2}{2g}} = \frac{\text{NPSH}_{ref} + (\Delta h_v)_{ref}}{\frac{V_{ref}^2}{2g}} \tag{4}$$

The inlet axial velocity V has been used instead of the rotative speed N to make the equation dimensionless. The velocity V is proportional to N thereby allowing this substitution. With the K-factor known, the cavitation performance of an inducer operated in a liquid without thermodynamic effects can be evaluated. The greater K-factor will result in the greater required NPSH.

One way to evaluate the thermodynamic effects of cavitation is to express the reference values in equation (2) as

$$\text{M-factor} = \left(\frac{\rho_v}{\rho_l}\right)_{ref} (\alpha_{ref}) \left(\frac{1}{V_{ref}}\right)^{0.8} \tag{5}$$

The axial velocity V is also used in this equation instead of the rotative speed N. With the substitution of equation (5), equation (2) will become

$$\left(\frac{\rho_v}{\rho_l}\right) = \text{M-factor} \left(\frac{1}{\alpha}\right) (V)^{0.8} \tag{6}$$

Equation (6) can then be used in conjunction with equation (1) or the curves of figure 5 to determine the Δh_v values for the conditions of interest. Thus, only the M-factor has to be known to qualitatively evaluate the magnitude of the thermodynamic effects of cavitation for various inducers at a fixed flow coefficient and head-rise-coefficient ratio. For a given temperature and rotative speed, the thermodynamic effects are proportional to the M-factor.

The cavitation parameters, M-factor and K-factor, are plotted in figure 13 as functions of flow coefficient for the three inducers. The parameters are presented for the flow coefficient range for which cavitation data were available. For the 80.6° and 84° inducers, the M-factor decreased with increasing flow coefficient. For the 78° inducer, the M-factor increased with increasing flow coefficient. The magnitude of

the M-factor is much smaller for the 78° inducer than for either the 80.6° or 84° inducer.

For the 84° inducer, the K-factor decreased and then increased with increasing flow coefficient. For both the 78° and 80.6° inducers, the K-factor increased with increasing flow coefficient.

Because the inducers were tested over different flow ranges, the cavitation parameters are also compared in figure 12 on the basis of a flow coefficient ratio. The flow coefficient corresponding to the tangent of the blade leading-edge fairing angle was used as the reference flow coefficient for these comparisons. For a given flow coefficient ratio, both M-factor and K-factor decreased with decreasing helix angle.

For the inducers tested, the through-flow area increases as the helix angle is decreased. Thus the size of the vapor cavity corresponding to a head-rise-coefficient ratio of 0.70 should also increase as the helix angle is decreased. This larger vapor cavity allows a reduction in the inlet pressure. Therefore, the decreasing pressure requirements (as indicated by a decreasing K-factor) with decreasing helix angle may be expected.

Comparison with Water Results

The three inducers operated in liquid hydrogen exhibit the same trends as did three similar inducers operated in water (ref. 1). The three inducers in reference 1 were compared on the basis of a cavitation number $\bar{k}$. The cavitation number $\bar{k}$ for a head-rise-coefficient ratio of 0.70 is shown in table II for both the water and hydrogen inducers. The results for both water and hydrogen tests show that the cavitation number was the smallest for the 84° inducer and largest for the 78° inducer.

The magnitude of the cavitation number is less for the hydrogen inducers than for the water inducers. This is attributed to the different way the leading edge of the hydrogen inducers were faired. The water inducers were faired to a wedge shape symmetrically about the blade centerline (ref. 1), and the hydrogen inducers were faired on the suction surface only (see fig. 2). It was indicated in reference 12 that lower cavitation numbers could be obtained by fairing the blade leading edges in the manner that the hydrogen inducers were faired.

SUMMARY OF RESULTS

The thermodynamic effects of cavitation for a 78° helical inducer were determined and compared with those obtained for 80.6° and 84° helical inducers. The noncavitation

and cavitation performances of the three inducers were also compared. The experimental inducers were tested over a liquid temperature range of 15.5 to 22.3 K (27.9° to 40.1° R) and a flow coefficient range of 0.058 to 0.130. This investigation yielded the following principal results:

1. The thermodynamic effects of cavitation for the 78° helical inducer increased with increasing liquid temperature, rotative speed, and flow coefficient. The magnitude of the thermodynamic effects varied from about 4 meters (13 ft) to about 33.5 meters (110 ft).

2. For a given flow coefficient ratio, the magnitude of the thermodynamic effects of cavitation was the greatest for the 84° inducer, and least for the 78° inducer.

3. For a given flow coefficient ratio, the pressure requirements as indicated by the cavitation parameter were also greatest for the 84° inducer and least for the 78° inducer.

4. The noncavitating flow range was the greatest for the 78° inducer and least for the 84° inducer. The noncavitating head-rise coefficient decreased with increasing flow coefficient for all three helical inducers.

Lewis Research Center,
National Aeronautics and Space Administration,
Cleveland, Ohio, February 17, 1971,
128-31.

APPENDIX - SYMBOLS

C_l	specific heat of liquid, J/(kg)(K); Btu/(lbm)(^{o} R)
dh_v/dT	slope of vapor pressure head to temperature curve, m/K; ft/^{o}R
g	acceleration due to gravity, m/sec^2; ft/sec^2
ΔH	pump head rise based on inlet density, m of liquid; ft of liquid
Δh_v	decrease in vapor pressure because of vaporization (magnitude of thermodynamic effect of cavitation), m of liquid; ft of liquid
K-factor	cavitation parameter, $(NPSH + \Delta h_v)/(V^2/2g)$
k	liquid thermal conductivity, J/(hr)(m)(K); Btu/(hr)(ft)(^{o}R)
$\bar{k}$	cavitation number, $(K\text{-factor} - 1)/\left(\frac{1}{\phi^2} + 1\right)$ or $\frac{(2g)(NPSH)}{U_t^2\,(1 + \varphi^2)} - \frac{\varphi^2}{(1 + \varphi^2)}$
L	latent heat of vaporization, J/kg; Btu/lbm
M-factor	cavitation parameter, $(\mathscr{V}_v/\mathscr{V}_l)_{ref}\ \alpha_{ref}\ (1/V_{ref})^{0.8}$, $(m^2/hr)(m/sec)^{-0.8}$; $(ft^2/hr)(ft/sec)^{-0.8}$
N	rotative speed, rpm
NPSH	net positive suction head (total pressure above vapor pressure), m of liquid; ft of liquid
U_t	blade tip speed, m/sec; ft/sec
V	average axial velocity at inducer inlet, m/sec; ft/sec
$\mathscr{V}_l$	volume of liquid involved in cavitation process, cm^3; in.^{3}
$\mathscr{V}_v$	volume of vapor, cm^3; in.^{3}
α	thermal diffusivity of liquid, $k/\rho_l C_l$, m^2/hr; ft^2/hr
ρ_l	density of liquid, kg/m^3; lbm/ft^3
ρ_v	density of vapor, kg/m^3; lbm/ft^3
ϕ	flow coefficient, V/U_t
ϕ_{le}	flow coefficient corresponding to tangent of blade leading-edge fairing angle
ψ	head-rise coefficient, $g\Delta H/U_t^2$
ψ/ψ_{NC}	cavitating-to-noncavitating head-rise-coefficient ratio

Subscripts:

NC noncavitating

ref reference value obtained from experimental tests

REFERENCES

1. Anderson, Douglas A.; Soltis, Richard F.; and Sandercock, Donald M.: Performance of 84° Flat-Plate Helical Inducer and Comparison with Performance of Similar 78° and 80.6° Inducers. NASA TN D-2553, 1964.

2. Meng, Phillip R.: Change in Inducer Net Positive Suction Head Requirement with Flow Coefficient in Low Temperature Hydrogen (27.9° to 36.6° R). NASA TN D-4423, 1968.

3. Ball, Calvin L.; Meng, Phillip R.; and Reid, Lonnie: Cavitation Performance of 84° Helical Pump Inducer Operated in 37° and 42° R Liquid Hydrogen. NASA TM X-1360, 1967.

4. Salemann, Victor: Cavitation and NPSH Requirements of Various Liquids. J. Basic Eng., vol. 81, no. 2, June 1959, pp. 167-180.

5. Spraker, W. A.: The Effects of Fluid Properties on Cavitation in Centrifugal Pumps. J. Eng. Power, vol. 87, no. 3, July 1965, pp. 309-318.

6. Ruggeri, Robert S.; and Moore, Royce D.: Method for Prediction of Pump Cavitation Performance for Various Liquids, Liquid Temperatures, and Rotative Speeds. NASA TN D-5292, 1969.

7. Moore, Royce D.; and Meng, Phillip R.: Thermodynamic Effects of Cavitation of an 80.6° Helical Inducer Operated in Hydrogen. NASA TN D-5614, 1970.

8. Moore, Royce D.; and Meng, Phillip R.: Effect of Blade Leading Edge Thickness on Cavitation Performance of 80.6° Helical Inducer in Hydrogen. NASA TN D-5855, 1970.

9. Moore, Royce D.; Ruggeri, Robert S.; and Gelder, Thomas F.: Effects of Wall Pressure Distribution and Liquid Temperature on Incipient Cavitation of Freon-114 and Water in Venturi Flow. NASA TN D-4340, 1968.

10. Meng, Phillip R.; and Moore, Royce D.: Cavitation and Noncavitation Performance of 78° Helical Inducer in Hydrogen. NASA TM X-2131, 1970.

11. Moore, Royce D.; and Meng, Phillip R.: Cavitation Performance of Line-Mounted 80.6° Helical Inducer in Hydrogen. NASA TM X-1854, 1969.

12. Stripling, L. B.; and Acosta, A. J.: Cavitation in Turbopumps - Part 1. J. Basic Eng., vol. 84, no. 3, Sept. 1962, pp. 326-338.

13. Meng, Phillip R.; and Moore, Royce D.: Cavitation Performance of 80.6° Helical Inducer in Liquid Hydrogen. NASA TM X-1808, 1969.

14. Meng, Phillip R.; and Moore, Royce D.: Hydrogen Cavitation Performance of 80.6° Helical Inducer Mounted in Line with Stationary Centerbody. NASA TM X-1935, 1970.

TABLE I. - GEOMETRIC DETAILS OF TEST INDUCERS

Design details	78° Helical inducer	80.6° Helical inducer	84° Helical inducer
Tip helix angle (from axial direction), deg	78	80.6	84
Rotor tip diameter, cm; in.	12.649; 4.980	12.649; 4.980	12.664; 4.986
Rotor hub diameter, cm; in.	6.294; 2.478	6.294; 2.478	6.294; 2.478
Hub-tip ratio	0.498	0.498	0.497
Number of blades	3	3	3
Axial length, cm; in.	5.08; 2.00	5.08; 2.00	5.08; 2.00
Peripheral extent of blades, deg	240	280	440
Tip chord length, cm; in.	26.47; 10.42	31.37; 12.35	48.62; 19.14
Hub chord length, cm; in.	13.00; 5.12	16.15; 6.36	24.16; 9.51
Solidity at tip	1.856	2.350	3.838
Tip blade thickness, cm; in.	0.254; 0.100	0.254; 0.100	0.170; 0.067
Hub blade thickness, cm; in.	0.483; 0.190	0.381; 0.150	0.254; 0.100
Calculated radial tip clearance at hydrogen temperature, cm; in.	0.064; 0.025	0.064; 0.025	0.064; 0.025
Ratio of tip clearance to blade height	0.020	0.020	0.020
Blade leading edge fairing angle, deg	6.0	4.7	3.0

TABLE II. - COMPARISON OF CAVITATION NUMBERS FOR INDUCERS OPERATING IN HYDROGEN AND IN WATER[a]

Inducer	Flow coefficient	Operation in -	Cavitation number, $\bar{k}$
84°	0.065	Water	0.0240
		Hydrogen	.0117
80.6°	0.095	Water	0.0268
		Hydrogen	.0177
78°	0.125	Water	0.0341
		Hydrogen	.0228

[a]Water cavitation numbers from ref. 1.

C-69-695

(a) 78° helical inducer.

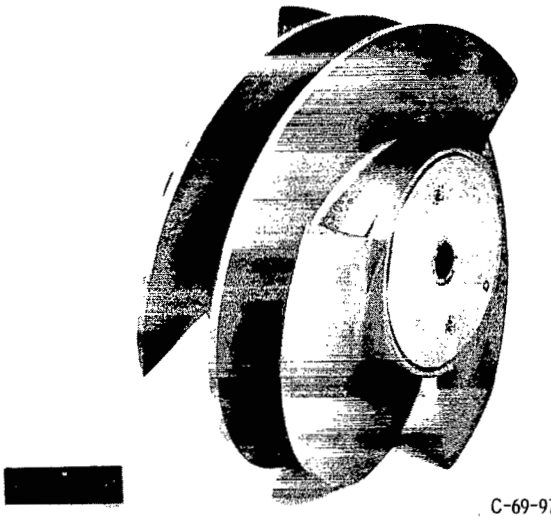

C-69-977

(b) 80.6 ° helical inducer.

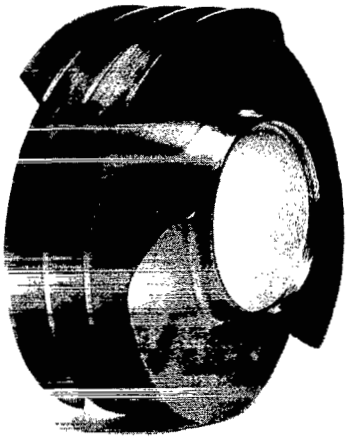

C-67-423

(c) 84° helical inducer.

Figure 1. - Test inducers.

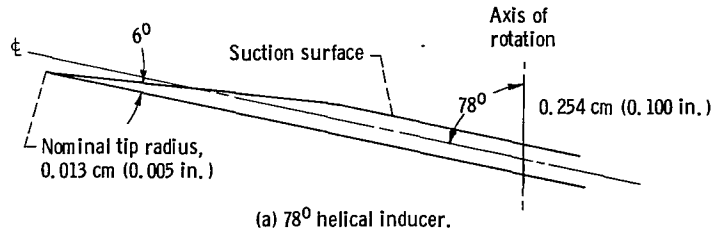

(a) 78° helical inducer.

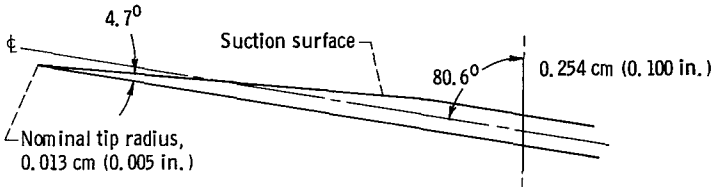

(b) 80.6° helical inducer.

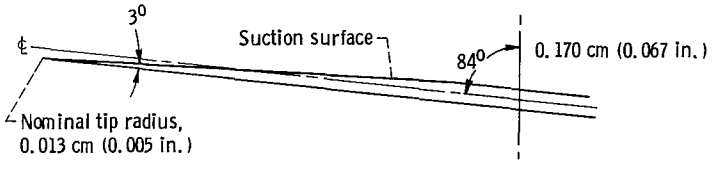

(c) 84° helical inducer.

Figure 2. - Inducer leading edge geometry.

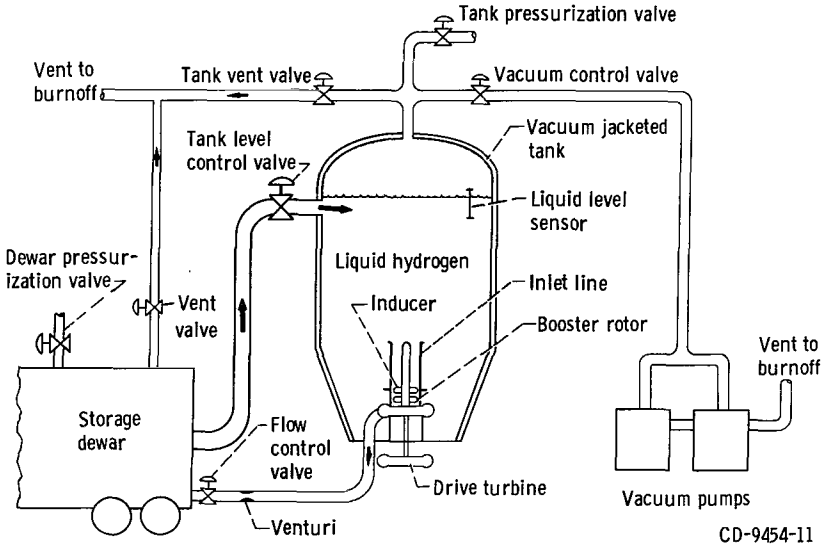

Figure 3. - Liquid-hydrogen pump test facility.

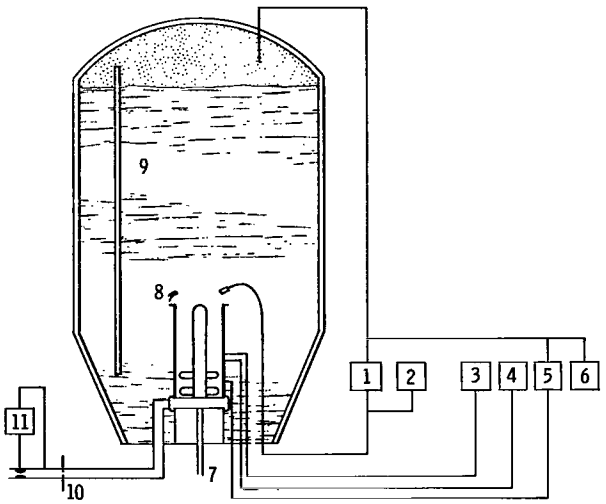

Item number	Parameter	Estimated system accuracy	Number used	Remarks
1	Tank net positive suction head	Low range ±0.05 psi (0.035 N/cm^2) High range ±0.25 psi (0.17 N/cm^2)	1 1	Measured as differential pressure (converted to head of liquid) between vapor bulb at line inlet and tank pressure corrected to line inlet conditions
2	Vapor pressure at line inlet	±0.25 psi (0.17 N/cm^2)	1	Vapor bulb charged with liquid hydrogen from research tank
3	Static pressure (line)	±0.05 psi (0.035 N/cm^2)	1	Average of three pressure taps (120° apart) located 10.5 in. (26.7 cm) above inducer inlet
4	Total pressure (line)	±0.05 psi (0.035 N/cm^2)	1	Shielded total pressure probe located 0.065 in. (0.165 cm) in from wall and 10.5 in. (26.7 cm) upstream at inducer
5	Inducer pressure rise	±1.0 psi (0.69 N/cm^2)	1	Shielded total pressure probe at midpassage 1 in. (2.54 cm) downstream of inducer
6	Tank pressure	±0.5 psi (0.35 N/cm^2)	1	Measured in tank ullage and corrected to inducer inlet conditions for reference pressure for differential transducers
7	Rotative speed	±150 rpm	1	Magnetic pickup in conjunction with gear on turbine drive shaft
8	Line inlet temperature	±0.1 R (0.06 K)	1	Platinum resistor probes 180° apart at inlet
9	Liquid level	±0.5 ft (0.15 m)	1	Capacitance gage, used for hydrostatic head correction to inducer inlet conditions
10	Venturi inlet temperature	+0.1 R (0.06 K)	1	Platinum resistor probe upstream of venturi
11	Venturi differential pressure	±0.25 psi (0.17 N/cm^2)	1	Venturi calibrated in air

Figure 4. - Instrumentation for liquid-hydrogen pump test facility.

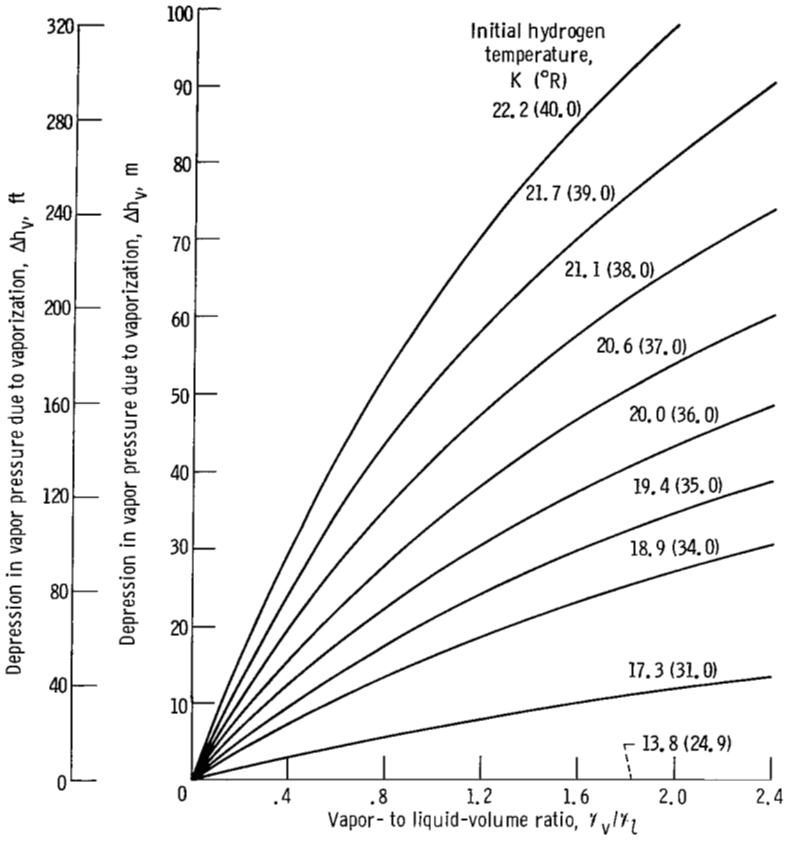

Figure 5. - Calculated vapor pressure depression due to vaporization as function of volume ratio for several liquid-hydrogen temperatures.

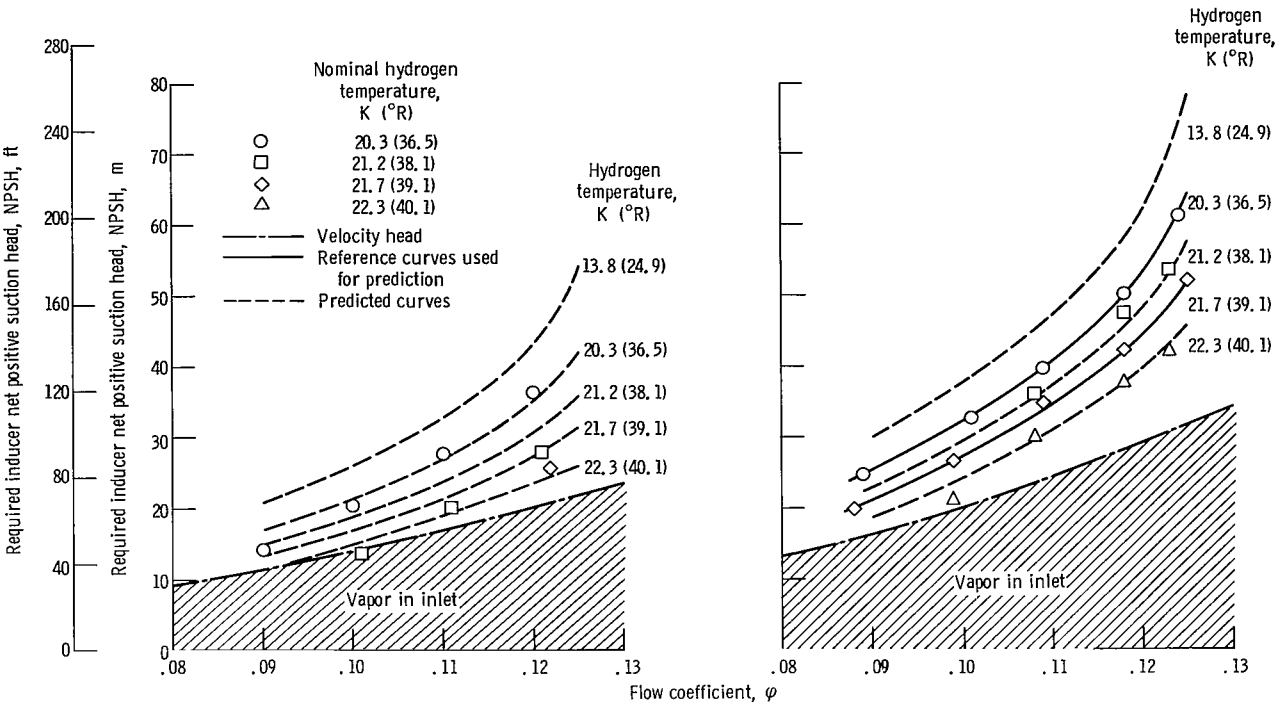

Figure 6. - Comparison of predicted and measured net positive suction head for 78° helical inducer in hydrogen. Head-rise-coefficient ratio, 0.70.

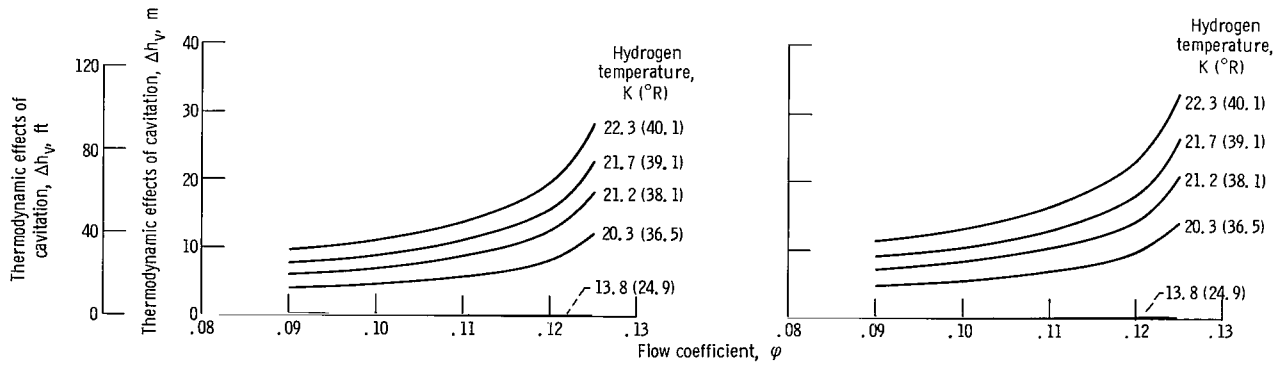

Figure 7. - Predicted thermodynamic effects of cavitation as function of flow coefficient for several hydrogen temperatures for 78° helical inducer. Head-rise-coefficient ratio, 0.70.

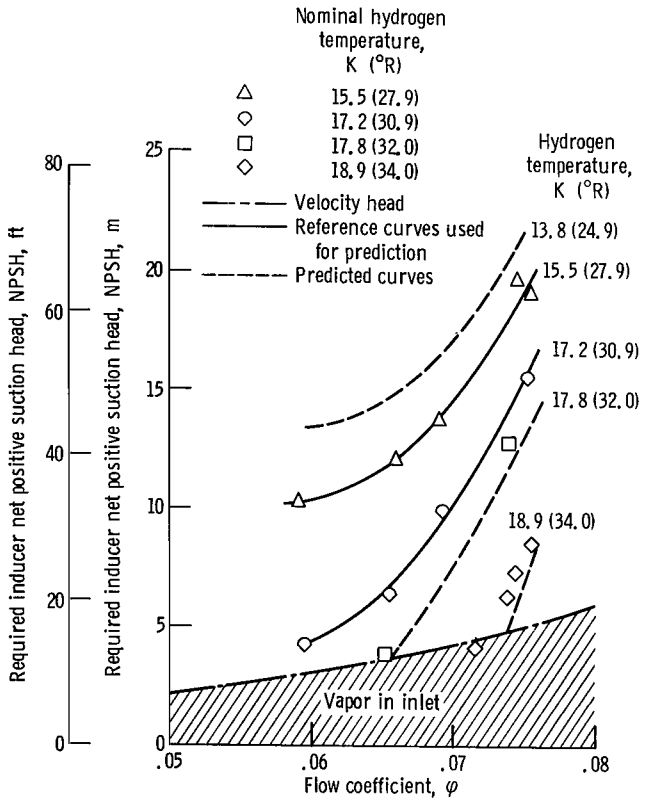

Figure 8. - Comparison of predicted and measured inducer net positive suction head for 84° helical inducer in hydrogen. Rotative speed, 20 000 rpm; head-rise-coefficient ratio, 0.70.

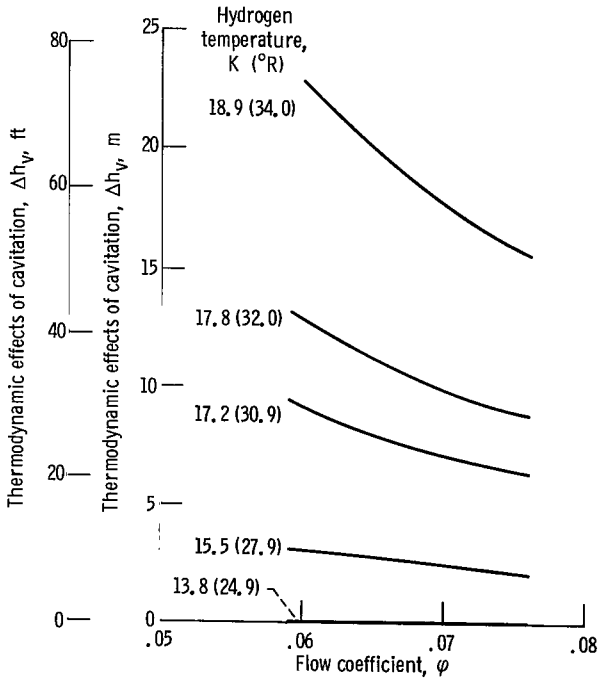

Figure 9. - Predicted thermodynamic effects of cavitation as function of flow coefficient for several hydrogen temperatures for 84° helical inducer. Rotative speed, 20 000 rpm; head-rise-coefficient-ratio, 0.70.

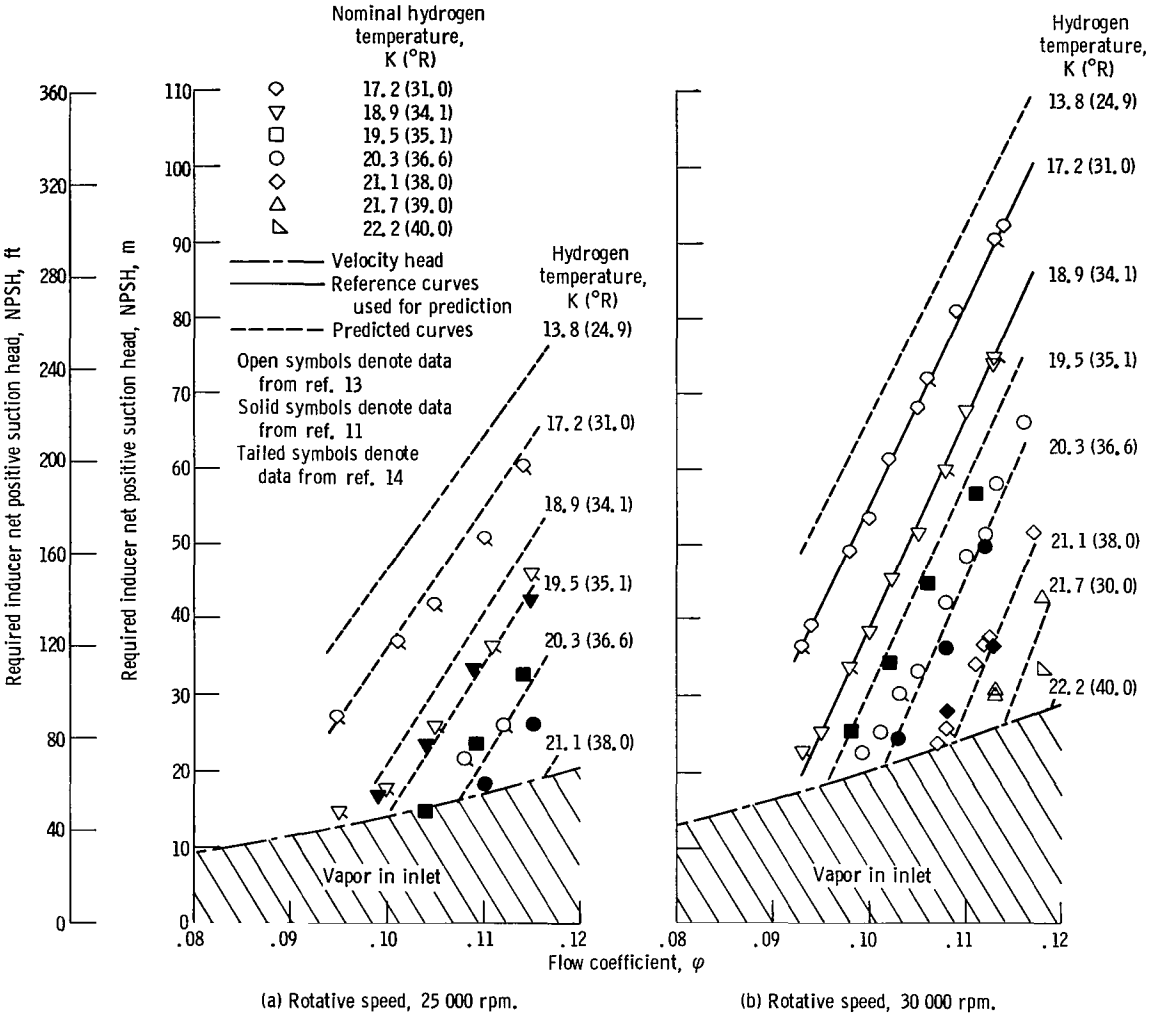

Figure 10. - Comparison of predicted and measured net positive suction head for 80.6° helical inducer in hydrogen. Head-rise-coefficient ratio, 0.70.

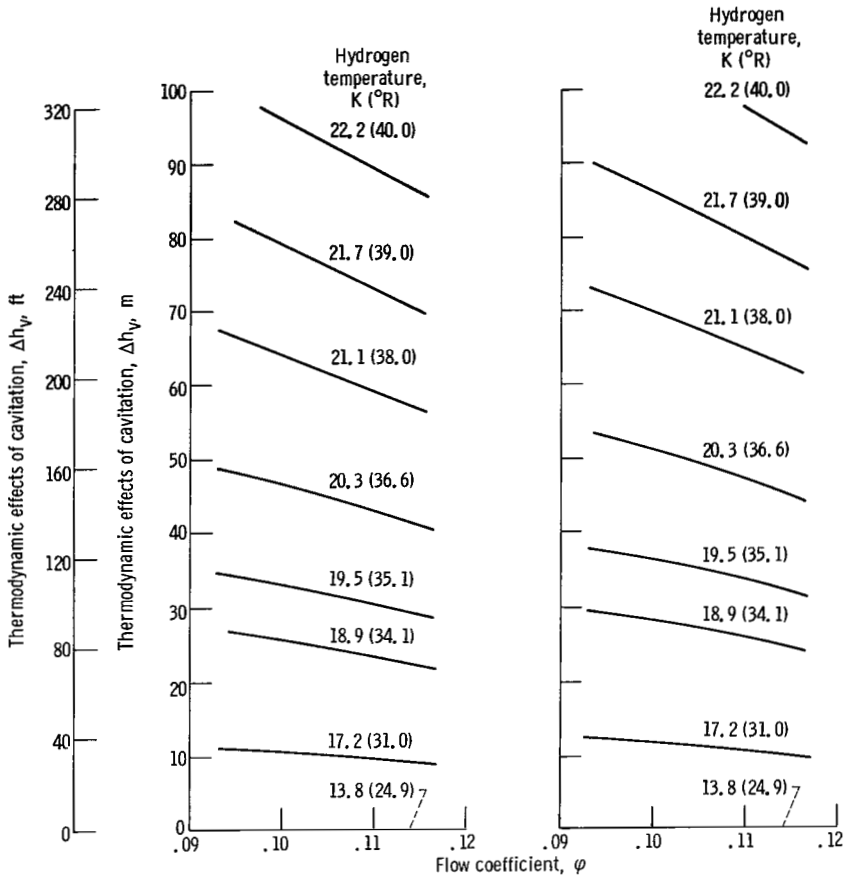

Figure 11. - Predicted thermodynamic effects of cavitation as function of flow coefficient for several hydrogen temperatures for 80.6° helical inducer. Head-rise-coefficient ratio, 0.70.

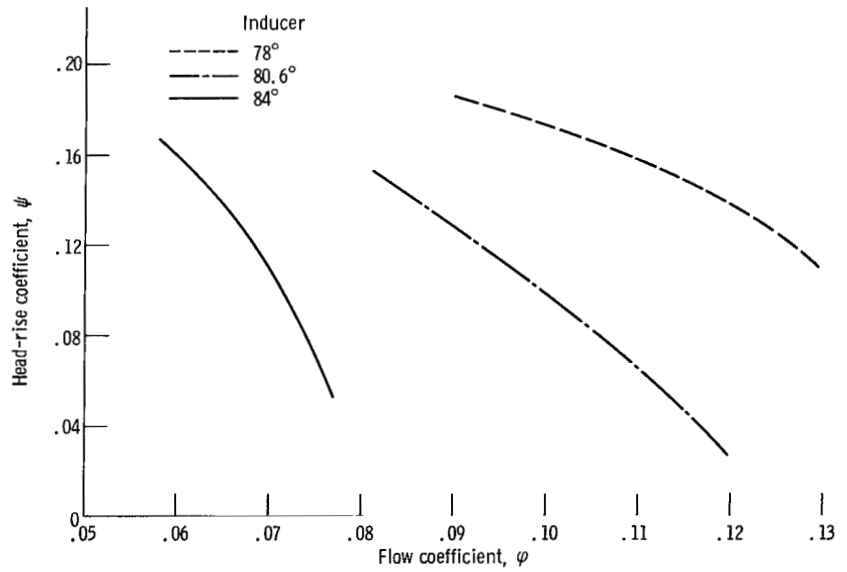

Figure 12. - Comparison of the noncavitating performances of three helical inducers.

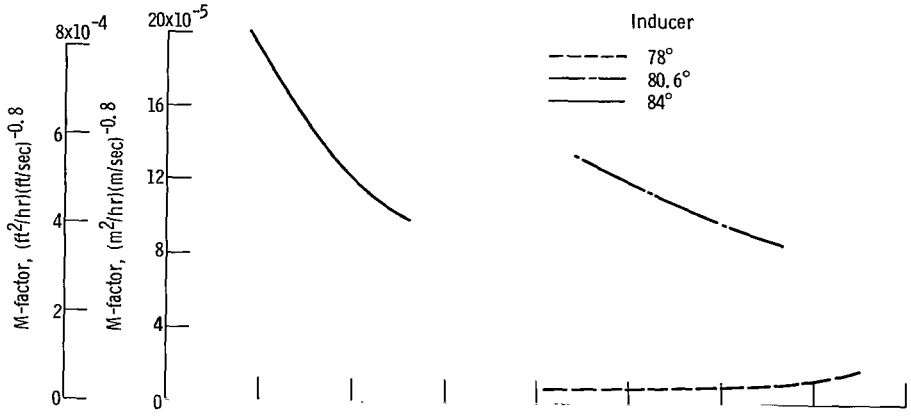

(a) M-factor.

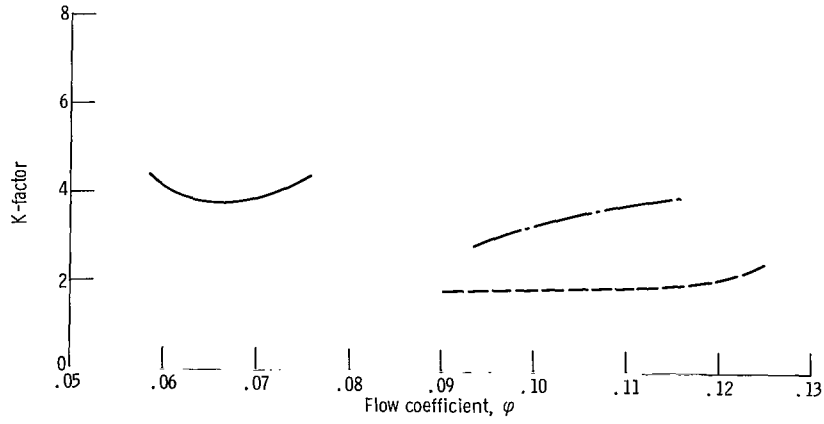

(b) K-factor.

Figure 13. - Comparison of the cavitation parameters for three helical inducers. Head-rise-coefficient ratio, 0.70.

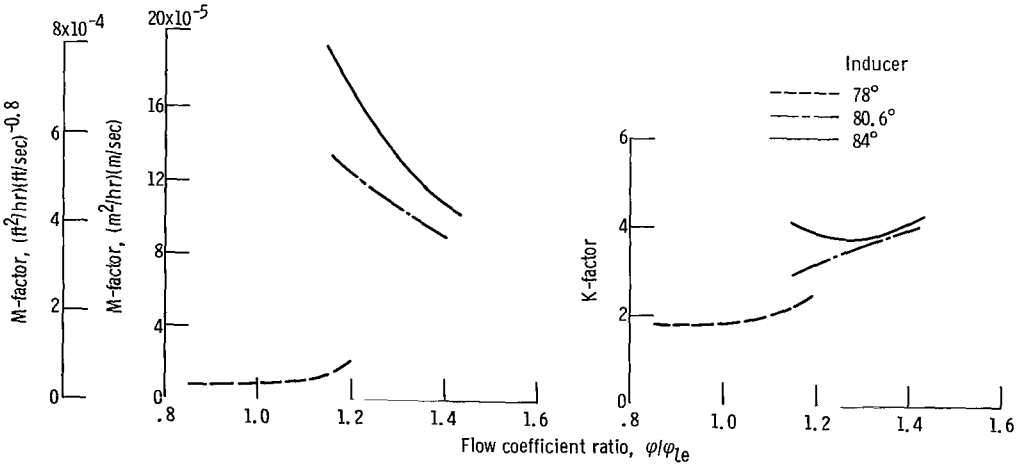

(a) M-factor.

(b) K-factor.

Figure 14. - Normalized cavitation performance.

05U 001 37 51 3DS 71.10 00903
AIR FORCE WEAPONS LABORATORY /WLOL/
KIRTLAND AFB, NEW MEXICO 87117

ATT E. LOU BOWMAN, CHIEF,TECH. LIBRARY

"The aeronautical and space activities of the United States shall be conducted so as to contribute . . . to the expansion of human knowledge of phenomena in the atmosphere and space. The Administration shall provide for the widest practicable and appropriate dissemination of information concerning its activities and the results thereof."

—NATIONAL AERONAUTICS AND SPACE ACT OF 1958

NASA SCIENTIFIC AND TECHNICAL PUBLICATIONS

TECHNICAL REPORTS: Scientific and technical information considered important, complete, and a lasting contribution to existing knowledge.

TECHNICAL NOTES: Information less broad in scope but nevertheless of importance as a contribution to existing knowledge.

TECHNICAL MEMORANDUMS: Information receiving limited distribution because of preliminary data, security classification, or other reasons.

CONTRACTOR REPORTS: Scientific and technical information generated under a NASA contract or grant and considered an important contribution to existing knowledge.

TECHNICAL TRANSLATIONS: Information published in a foreign language considered to merit NASA distribution in English.

SPECIAL PUBLICATIONS: Information derived from or of value to NASA activities. Publications include conference proceedings, monographs, data compilations, handbooks, sourcebooks, and special bibliographies.

TECHNOLOGY UTILIZATION PUBLICATIONS: Information on technology used by NASA that may be of particular interest in commercial and other non-aerospace applications. Publications include Tech Briefs, Technology Utilization Reports and Technology Surveys.

Details on the availability of these publications may be obtained from:

SCIENTIFIC AND TECHNICAL INFORMATION OFFICE

NATIONAL AERONAUTICS AND SPACE ADMINISTRATION

Washington, D.C. 20546